

Fermi surface pockets in ortho-II $\text{YBa}_2\text{Cu}_3\text{O}_{6.5}$: the origin of quantum oscillations?

A. Carrington, and E.A. Yelland

H.H. Wills Physics Laboratory, University of Bristol, Tyndall Avenue, Bristol, United Kingdom.

(Dated: February 8, 2022)

In this paper we explore whether the quantum oscillation signals recently observed in ortho-II $\text{YBa}_2\text{Cu}_3\text{O}_{6.5}$ (OII-Y123) may be explained by conventional density functional band-structure theory. Our calculations show that the Fermi surface of OII-Y123 is extremely sensitive to small shifts in the relative positions of the bands. With rigid band shifts of around ± 30 meV small tubular pockets of Fermi surface develop around the Y point in the Brillouin zone. The cross-sectional areas and band masses of the quantum oscillatory orbits on these pockets are close to those observed. The differences between the band-structure of OII-Y123 and $\text{YBa}_2\text{Cu}_4\text{O}_8$ (Y124) are discussed with reference to the very recent observation of quantum oscillations in Y124.

The nature of the normal state of the high temperature cuprate superconductors (HTC) has been a topic of intense discussion ever since their discovery. The unusual temperature dependence shown by the resistivity and Hall coefficient for example, and how these evolve as a function of doping, has led to a wide range of exotic theories of the nature of the normal state.¹ Many of these theories depart substantially from the standard Fermi liquid model of a metal, particularly in the underdoped region of the phase diagram.

The recent report² of the observation of Shubnikov-de Haas (SdH) oscillations in the Hall and longitudinal resistivities of underdoped ortho-II $\text{YBa}_2\text{Cu}_3\text{O}_{6.5}$ (OII-Y123) was a surprising and potentially extremely important result. These oscillations suggest that even in the underdoped region some well-defined pockets of Fermi surface exist. The observed orbits have a frequency of $\sim 530 \pm 20$ T and a mass, $m^* = 1.9 \pm 0.1m_e$ (m_e is the free electron mass). A single pocket with this dHvA frequency corresponds to a small ($\sim 2\%$) fraction of the Brillouin zone. Identifying the origin of this orbit is clearly very important for its interpretation. In this paper, we discuss whether the SdH signals could come from small pockets of Fermi surface predicted by conventional density functional band-structure calculations.

Our understanding of the electronic structure of the cuprates has, to date, mostly been led by angle resolved photoemission spectroscopy (ARPES). The resolution of this technique has advanced rapidly over the past decade and had provided many key insights into the physics of HTC.³ More recently, the strong angle dependent magnetoresistance of strongly overdoped $\text{Tl}_2\text{Ba}_2\text{CuO}_{6+\delta}$ has been used to extract information about the Fermi surface and scattering rate.^{4,5} The shape and size of the Fermi surfaces measured by both these techniques are generally in very good agreement with conventional density functional theory (DFT) band-structure calculations.^{3,6}

Quantum oscillatory effects, e.g. the de Haas-van Alphen (dHvA) and Shubnikov-de Haas effects, are very powerful probes of the Fermi surface properties of a metal. Unlike ARPES, they probe the bulk of the material (and so are not sensitive to surface defects) and are a true three dimensional probe of the quasiparticles at the Fermi level. The analysis of the amplitude and

frequency of the signals and how these change as a function of magnetic field and temperature, gives information about the Fermi surface and the quasiparticle masses and scattering rates. The main constraint is that impurities severely attenuate the SdH/dHvA signal, according to the Dingle factor $R_D = \exp(-\frac{\pi\hbar k_F}{eB\ell})$ (here $\pi k_F^2 = \mathcal{A}$ the cross-sectional area of the dHvA orbit and ℓ is the orbitally averaged mean free path). The small size of the orbit in OII-Y123 was a key factor in it being observable.

Band-structure calculations of fully oxygenated ortho-I $\text{YBa}_2\text{Cu}_3\text{O}_7$ (OI-Y123) show a small tubular pocket of Fermi surface near the S point which derives from the ‘CuO chain bands’^{7,8,9} (see below). This could be a simple explanation for the origin of the observed SdH orbit. However the band-structure calculations of Bascones *et al.*¹⁰ indicate that this small pocket is absent in OII-Y123. Another intriguing possibility is that the SdH signal comes from pockets close to the nodal regions, which may have formed because of Fermi surface reconstruction. In this paper we calculate the band-structure of OII-Y123 using conventional density functional theory techniques and investigate the possible extremal orbits which could give rise to the observed orbit. We contrast this with similar calculations on the double-chain cuprate $\text{YBa}_2\text{Cu}_4\text{O}_8$ (Y124) in which SdH oscillations have also recently been observed.^{11,12}

Our calculations were carried out using the Wien2K package,¹³ which is an implementation of a full-potential, augmented plane wave plus local orbital scheme. We used a generalized gradient approximation form for the exchange correlation potential,^{14,15} and the crystal structure of $\text{YBa}_2\text{Cu}_3\text{O}_{6.5}$ determined by Grybos *et al.*^{16,17} A dense k -mesh of $\sim 10^4$ points in the full Brillouin zone ($19 \times 39 \times 12$, or 1400 points in the irreducible wedge of the Brillouin zone) was used for the self-consistency cycle.

The calculated band-structure in the basal plane at the center of the Brillouin zone ($k_z = 0$) is shown in Fig. 1. The main features can be easily related to that of fully oxygenated OI-Y123 by band folding. In the first panel of the Fig. 1(a) we show our calculation of the band-structure of OI-Y123 which is almost identical to previous calculations (e.g., Refs.7,9). The OI results have then been folded down into the smaller OII Brillouin zone produced by doubling the a lattice parameter (panel b).

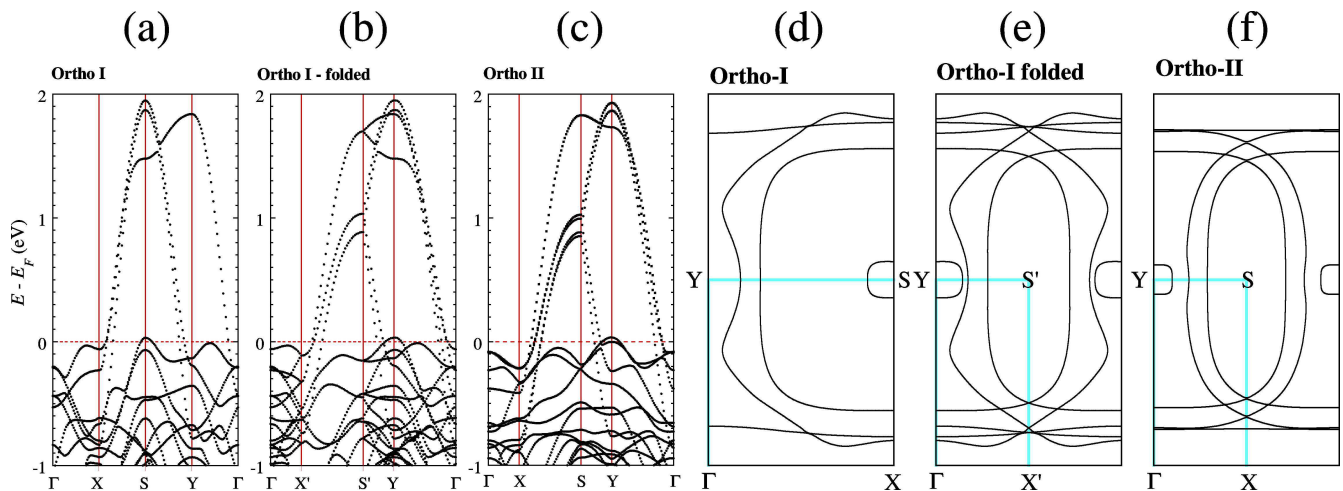


FIG. 1: (Color online) Panels (a-c): The band-structure of $\text{YBa}_2\text{Cu}_3\text{O}_{7-\delta}$. (a) OI-Y123, (b) OI-Y123 folded in to the reduced zone of OII-Y123 (c) OII-Y123. Panels (d-f) Fermi surfaces of $\text{YBa}_2\text{Cu}_3\text{O}_{7-\delta}$. (d) OI-Y123, (e) OI-Y123 folded, (f) OII-Y123 (with $\Delta E_F = +20$ meV).

It can be seen that this procedure reproduces many of the features of the full OII-Y123 calculation (panel c). The effect of the band folding on the Fermi surface is also shown in the figure and again compared to the results from the OII-Y123 calculation (panels d-f).

Moving along the X-S line the first band to cross the Fermi level is mainly due to the CuO chain (Fig. 1c). It can be seen that this is very close to being one-dimensional and has much less dispersion compared to the OI result. Note that there is only one chain band crossing in the OII calculation compared to two in the folded OI calculation because OII only has one conducting CuO chain per unit cell. The next four crossings are due to the CuO_2 planes. As in the OI calculation there is a sizeable splitting between the bonding and antibonding CuO_2 bands (~ 210 meV along the X-S line at E_F). Each of these two bands are further split into two by the additional $2a$ periodicity. This is most evident close to the S point. We find that this splitting is very small at E_F along the X-S line, being $\sim 17 \pm 2$ meV. In the OI-Y123 calculation a fairly flat CuO/BaO band, arising mainly from hopping between chain oxygen sites via the apical O site in the BaO layer below it, passes through E_F close to the S point and gives rise to a small tubular (quasi-two-dimensional) hole pocket.^{8,9,18} Band folding moves this same pocket to the Y point in the small (OII) zone. In the full OII-Y123 calculation, this band also crosses E_F and again forms a tubular hole pocket close to the Y point. In addition, a second band with the same character is very close in energy, ~ 35 meV lower at Y.

Our results are similar to a calculation of OII-Y123 reported by Bascones *et al.*¹⁰ The main differences are that the splittings of the CuO_2 bands due to the $2a$ periodicity are larger and near to Y the CuO/BaO bands are more closely spaced (and ~ 50 meV lower in energy) than in our calculation. Bascones *et al.* used a TB-LMTO-ASA method which may be less accurate for a non-close

packed structure like OII-Y123 than the full potential method used here. In any case, these differences would not change our essential conclusions.

The shape and size of the two plane sheets predicted for OI-Y123 have been verified by ARPES measurements on $\text{YBa}_2\text{Cu}_3\text{O}_{6.95}$.¹⁹ There is also some weak evidence for the quasi-1D chain sheet but there is no sign of the hole pocket centered on S. However, it should be mentioned that ARPES measurements on YBCO are complicated by a surface feature originating from the CuO chains, which may limit the resolution for Fermi surface sheets with significant chain character.¹⁹

Although DFT calculations usually correctly describe the general features of the band-structure, there are often small discrepancies with respect to the relative positions of the bands when compared to experiment. This is true even if the calculation has been converged to the meV level. Sr_2RuO_4 is an example of an oxide material, with a similar structure to the cuprate superconductor $\text{La}_{2-x}\text{Sr}_x\text{CuO}_4$, which has been studied in detail by dHvA measurements. To get agreement with band-structure calculations the bands need to be shifted by ~ 40 meV, in opposite directions.²⁰ Even in the relatively simple material MgB_2 , shifts of order 100 meV are needed.^{21,22}

In Fig. 2 we show how the Fermi surface of OII-Y123 changes as the E_F is varied by ± 35 meV. These small rigid band shifts correspond to adding (removing) 0.05 (0.07) electrons per Cu atom, although a similar result could be obtained without doping by moving the plane and chain bands in opposite directions. For $\Delta E_F = +35$ meV the Fermi surface consists of two large hole-like tubular CuO_2 sheets centered on S, plus three quasi-one-dimensional sheets (one from the chains and two from the planes). As E_F is reduced a small hole-like pocket develops near the Y point, the origin of which (as discussed above) is the same as that of the pocket near

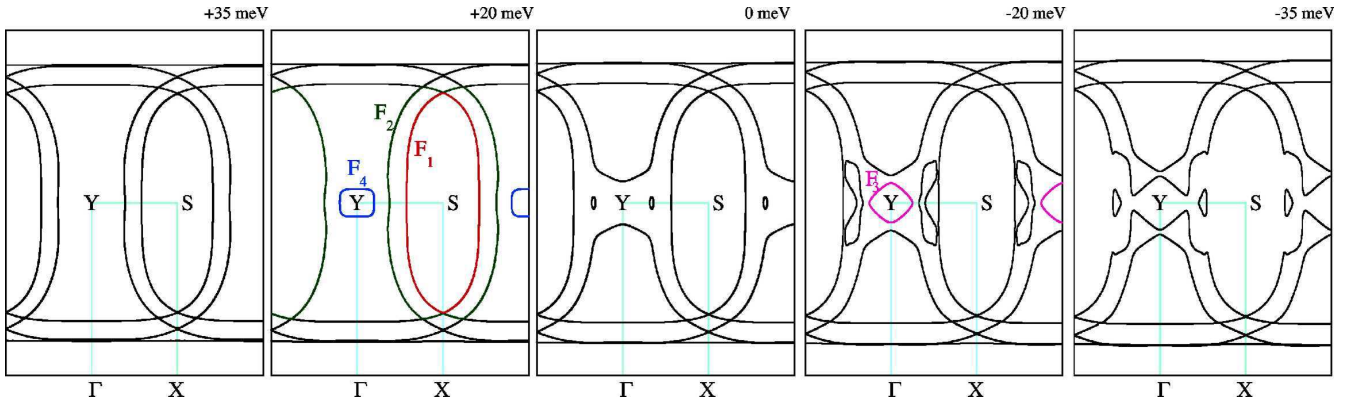


FIG. 2: (Color online) Evolution of the Fermi surface of OII-YBa₂Cu₃O_{6.5} with Fermi level shift ΔE_F . The figure shows two-dimensional cuts within the basal plane ($k_z = 0$), as indicated by the symmetry labels. The primary quantum oscillation orbits (F_n) are marked on the +20 meV and -20 meV panels.

the S point in OI-Y123. Further reduction of E_F results in this pocket growing in size and then merges with the antibonding CuO₂ plane sheet. As E_F is further reduced the second CuO/BaO band passes through the Fermi level giving rise to another pocket. Eventually this merges with the bonding CuO₂ plane sheet. Both of the pockets that open close to Y are quasi-two-dimensional (tubular) sheets, with relatively weak warping along the c direction (see Fig. 3). Similar results to these have recently been report by Elfimov *et al.*²³

The above illustrates the extreme sensitivity of the Fermi surface to the relative positions of the bands and means that subtle changes to the doping could result in small Fermi surface pockets being formed. It is possible that one such pocket could give rise to the quantum oscillation signals observed by Doiron-Leyraud *et al.*² To investigate this possibility more fully we have calculated the quantum oscillation frequencies [$F = (\hbar/2\pi e)\mathcal{A}$] and band masses [$m_b = \frac{\hbar^2}{2\pi} \frac{\partial \mathcal{A}}{\partial E}$]. The frequencies shown in the bottom panel of Fig. 4 (F_3 and F_4) are from the small hole pockets discussed above, whereas those in the up-

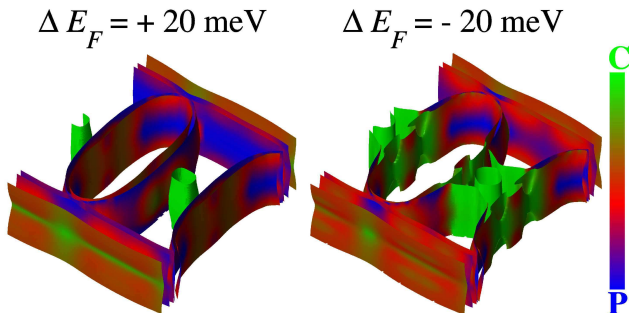


FIG. 3: (Color online) Three dimensional image of the calculated Fermi surface of OII-Y123 showing the small pockets centered on the Y points for the two different Fermi level shifts indicated. The shading indicates the band character C=Chain like (including apical oxygen), P=plane like.

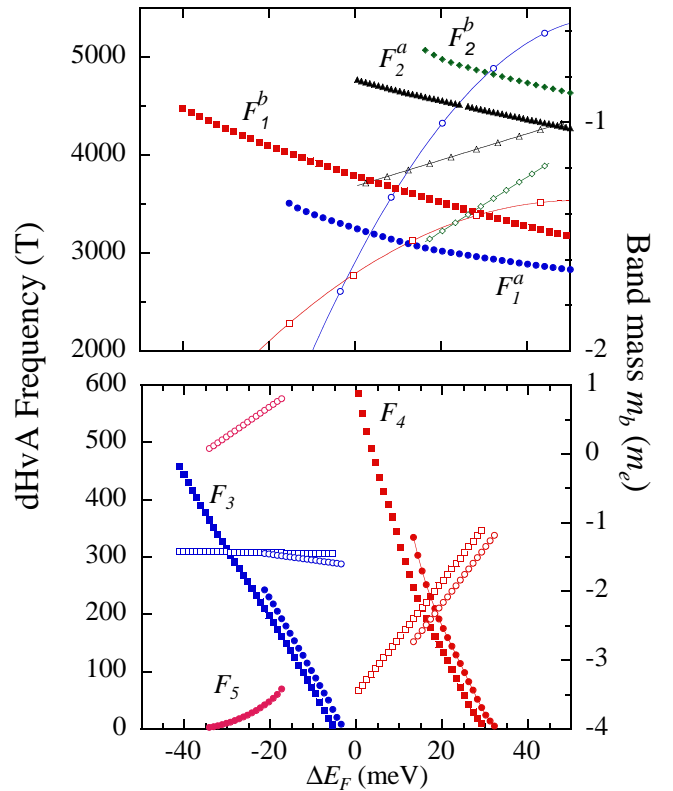


FIG. 4: (Color online) Extremal dHvA frequencies versus Fermi level shift (solid symbols). The corresponding band masses are shown with open symbols (right-hand axis).

per panel (F_1 and F_2) are from the main CuO₂ sheet surfaces. Each of the tubular sections of Fermi surface has a minimum and maximum extremal area which have been labeled F_i^a and F_i^b respectively in the figure. As expected, the extremal areas (dHvA frequencies) of both hole pockets vary strongly with the Fermi level shift and have maximum frequencies of 400-600 T. The band mass of the pocket F_3 is roughly constant as a function of

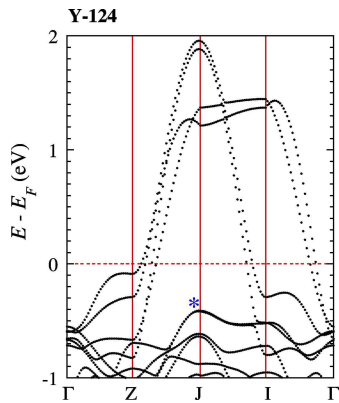


FIG. 5: (Color online) Band-structure of $\text{YBa}_2\text{Cu}_4\text{O}_8$ (Y124). The symmetry labels appropriate for the Ammm space group of Y124 are the same as in Ref.24. The path ΓZJI is approximately equivalent to the ΓXSJ path used in the other figures for the Pmmm space group of OI/II-Y123.

ΔE_F with an average value of $\sim 1.5 m_e$. The mass of the other pocket orbit, F_4 is much more variable, ranging from ~ 1.5 for large ΔE_F to ~ 3 as ΔE_F approaches zero. A similar calculation for OI-Y123 was reported in Ref.18.

The experimentally observed orbit frequency ($F = 530 \pm 20$ T) is at the upper limit of the calculated range for both F_3 and F_4 . The observed mass of the orbit ($m^* = 1.9 \pm 0.1 m_e$) seems to be more compatible with F_3 than F_4 . We expect that the observed quasiparticle mass should be enhanced compared to the band mass [$m^* = (1 + \lambda)m_b$] because of many body interactions (electron-phonon and electron-electron) which are not included in the present calculations. Although it is expected that λ will be relatively large ($\sim 1 - 2$) on the CuO_2 planes²⁵ it could be substantially less on these

sheets of Fermi surface without significant plane character. Hence, the calculated mass of F_3 could be consistent with experiment. Experimental studies of the pressure or doping dependence of the SdH frequencies in Y123 may help determine this interpretation is correct. An alternative approach is to study other cuprate materials where the CuO/BaO band is either absent or is at markedly different energies.

Very recently two groups^{11,12} have reported the observation of SdH oscillation in Y124 with a comparable frequency to those in OII-Y123. Y124 is an intrinsically underdoped cuprate with a similar structure to OI-Y123, but with a double chain layer and a doubled unit cell along the c -direction. Our calculations of the band-structure, which are essentially the same as reported previously,^{24,26} show that the CuO/BaO band which gives rise to the pockets in Y123 is now around 400 meV below E_F at the zone corner J (marked with an asterisk in Fig. 5). Hence, it is very unlikely that this band could be responsible for the experimental observations. In fact, we not find any orbits within $\Delta E_F = \pm 400$ meV which have frequencies close to experiment.

In summary, we have presented calculations of the electronic structure of OII-Y123, and have discussed possible origins of low frequency quantum oscillation signals. Two possible orbits, both arising from chain/apical oxygen bands have been identified, which with a small shift in the relative energies of the bands, have extremal areas compatible with the observed SdH signals. The band masses of the quasiparticles on at least one of these orbits is roughly consistent with those observed. It seems unlikely however that the reported orbits in Y124 can be explained by a similar band-structure approach.

We thank S.B. Dugdale, N.E. Hussey, and S.M. Hayden for useful comments.

¹ N. E. Hussey, *Normal State Transport Properties* (Springer - Holland, 2007), in 'Handbook of High Temperature Superconductivity: Theory and Experiment', by J. Brooks (Adapter), J. R. Schrieffer (Editor).
² N. Doiron-Leyraud, C. Proust, D. Leboeuf, J. Levallois, J. B. Bonnemaïson, R. X. Liang, D. A. Bonn, W. N. Hardy, and L. Taillefer, *Nature* **447**, 565 (2007).
³ A. Damascelli, Z. Hussain, and Z. X. Shen, *Rev. Mod. Phys.* **75**, 473 (2003).
⁴ N. E. Hussey, M. Abdel-jawad, A. Carrington, A. P. Mackenzie, and L. Balicas, *Nature* **425**, 814 (2003).
⁵ M. Abdel-jawad, M. P. Kennett, L. Balicas, A. Carrington, A. P. Mackenzie, R. H. Mckenzie, and N. E. Hussey, *Nat. Phys.* **2**, 821 (2006).
⁶ S. S. Sahrakorpi, H. Lin, R. Markiewicz, and A. Bansil, *cond-mat/0607132* (2006).
⁷ W. E. Pickett, R. E. Cohen, and H. Krakauer, *Phys. Rev. B* **42**, 8764 (1990).
⁸ W. E. Pickett, *Rev. Mod. Phys.* **61**, 433 (1989).
⁹ O. K. Andersen, A. I. Liechtenstein, O. Jepsen, and

F. Paulsen, *J. Phys. Chem. Solids* **56**, 1573 (1995).
¹⁰ E. Bascones, T. M. Rice, A. O. Shorikov, A. V. Lukoyanov, and V. I. Anisimov, *Phys. Rev. B* **71**, 012505 (2005).
¹¹ E. A. Yelland, J. Singleton, C. H. Mielke, N. Harrison, F. F. Balakirev, B. Dabrowski, and J. R. Cooper, *arXiv:0707.0057v1* [cond-mat.supr-con].
¹² A. F. Bangura, J. D. Fletcher, A. Carrington, J. Levallois, M. Nardone, B. Vignolle, P. J. Heard, N. Doiron-Leyraud, D. LeBoeuf, L. Taillefer, S. Adachi, C. Proust, and N. E. Hussey, *arXiv:0707.4461v1* [cond-mat.supr-con].
¹³ P. Blaha, K. Schwarz, G. K. H. Madsen, D. Kvasnicka, and J. Luitz, *WIEN2K, An Augmented Plane Wave + Local Orbitals Program for Calculating Crystal Properties* (Karlheinz Schwarz, Techn. Universität Wien, Austria, 2001), ISBN 3-9501031-1-2.
¹⁴ J. P. Perdew, K. Burke, and M. Ernzerhof, *Phys. Rev. Lett.* **77**, 3865 (1996).
¹⁵ The calculations were repeated using a local spin density approximation [W. Perdew and Y. Wang, *Phys. Rev. B* **45**, 13244 (1992)]. No significant differences were found.

- ¹⁶ J. Grybos, D. Hohlwein, T. Zeiske, R. Sonntag, F. Kubanek, K. Eichhorn, and T. Wolf, *Physica C* **220**, 138 (1994).
- ¹⁷ J. Grybos, M. Wabia, N. Guskos, and J. Typek, *Molecular Physics Reports* **34**, 121 (2001).
- ¹⁸ I. I. Mazin, O. Jepsen, O. K. Andersen, A. I. Liechtenstein, S. N. Rashkeev, and Y. A. Uspenskii, *Phys. Rev. B* **45**, 5103 (1992).
- ¹⁹ M. C. Schabel, C.-H. Park, A. Matsuura, Z.-X. Shen, D. A. Bonn, R. Liang, and W. N. Hardy, *Phys. Rev. B* **57**, 6090 (1998).
- ²⁰ A. P. Mackenzie, S. R. Julian, A. J. Diver, G. J. McMullan, M. P. Ray, G. G. Lonzarich, Y. Maeno, S. Nishizaki, and T. Fujita, *Phys. Rev. Lett.* **76**, 3786 (1996).
- ²¹ A. Carrington, P. J. Meeson, J. R. Cooper, L. Balicas, N. E. Hussey, E. A. Yelland, S. Lee, A. Yamamoto, S. Tajima, S. M. Kazakov, et al., *Phys. Rev. Lett.* **91**, 037003 (2003).
- ²² A. Carrington, E. A. Yelland, J. D. Fletcher, and J. R. Cooper, *Physica C* **456**, 92 (2007).
- ²³ I.S. Elfimov, G.A. Sawatzky, and A. Damascelli, arXiv:0706.4276v1 [cond-mat.str-el].
- ²⁴ C. Ambroschdraxl, P. Blaha, and K. Schwarz, *Phys. Rev. B* **44**, 5141 (1991).
- ²⁵ A. Lanzara, P. V. Bogdanov, X. J. Zhou, S. A. Kellar, D. L. Feng, E. D. Lu, T. Yoshida, H. Eisaki, A. Fujimori, K. Kishio, et al., *Nature* **412**, 510 (2001).
- ²⁶ J. J. Yu, K. T. Park, and A. J. Freeman, *Physica C* **172**, 467 (1991).